catalysts

MDPI

Review

Indoor Light Enhanced Photocatalytic Ultra-Thin Films on Flexible Non-Heat Resistant Substrates Reducing Bacterial Infection Risks

Sami Rtimi

Ecole Polytechnique Fédérale de Lausanne, EPFL-SB-ISIC-GPAO, Station 6, CH-1015 Lausanne, Switzerland; sami.rtimi@epfl.ch; Tel.: +41-21-693-6150

Academic Editor: Bunsho Ohtani
Received: 14 January 2017; Accepted: 7 February 2017; Published: 13 February 2017

Abstract: Photocatalytic antibacterial sol-gel coated substrates have been reported to kill bacteria under light or in the dark. These coatings showed non-uniform distribution, poor adhesion to the substrate and short effective lifetime as antibacterial surfaces. These serious limitations to the performance/stability retard the potential application of antibacterial films on a wide range of surfaces in hospital facilities and public places. Here, the preparation, testing and performance of flexible ultra-thin films prepared by direct current magnetron sputtering (DCMS) at different energies are reviewed. This review reports the recent advancements in the preparation of highly adhesive photocatalytic coatings prepared by up to date sputtering technology: High Power Impulse Magnetron Sputtering (HIPIMS). These latter films demonstrated an accelerated antibacterial capability compared to thicker films prepared by DCMS leading to materials saving. Nanoparticulates of Ti and Cu have been shown during the last decades to possess high oxidative redox potentials leading to bacterial inactivation kinetics in the minute range. In the case of TiO_2-CuO_x films, the kinetics of abatement of *Escherichia coli* (*E. coli*) and methicillin resistant *Staphylococcus aureus* (MRSA) were enhanced under indoor visible light and were perceived to occur within few minutes. Oligodynamic effect was seen to be responsible for bacterial inactivation by the small amount of released material in the dark and/or under light as detected by inductively-coupled plasma mass spectrometry (ICP-MS). The spectral absorbance (detected by Diffuse Reflectance Spectroscopy (DRS)) was also seen to slightly shift to the visible region based on the preparation method.

Keywords: catalytic thin films; sputtering; bacterial inactivation; surface characterization; metal oxides; interfacial charge transfer (IFCT); nanoparticulates

1. Introduction

Hospital acquired infection (HAI) is a topic of increasing attention due to the increasing number of incidents reported at the national or international levels. Many approaches were adopted to try to reduce the risks of infections in hospital facilities, schools and public places. The majority of these approaches were shortcut due to their short operational time or the development of bacterial resistance to their active ingredients. During the last decade, sol-gel antimicrobial films/coatings are drawing more and more attention since they have been shown to reduce or preclude the formation of infectious bacteria and biofilms [1–4]. More effective antibacterial films are needed due to the increasing bacterial resistance to commercial antibiotics applied on flat or multifaceted shape surfaces [5]. Consequently, healthcare acquired infections (HAIs) are becoming more frequent. This progresses into a grave problem and is also leading to increasing healthcare costs. To preclude/decrease HAIs, many studies [6,7] have reported on the antibacterial capability of impregnated textiles in

Cu-suspensions. Further, colloidal Cu-coated textiles have been prepared and tested to preclude numerous pathogens [8,9].

Several journals have recently reported TiO_2 films and dispersions leading to pathogen inactivation [10–14]. During the last five decades, antibacterial Ag-colloids have been extensively studied describing the antibacterial activity of Ag-impregnated textiles [15,16]. These colloidal/sol-gel preparations are not mechanically stable, non-reproducible, show low uniformity and tiny adhesion to the substrate [17]. This moved many research laboratories towards the preparation of more adhesive antibacterial films to overcome the inadequacies of colloidal coated films on diverse substrates.

Recently, many research groups [18–22] have reported antibacterial coatings based on Ag, Cu and TiO_2 on different substrates by Chemical Vapor Deposition (CVD) and Physical Vapor Depositions (PVD) techniques. Both techniques are used to produce high-purity and high-uniformity solid materials. Most coating studies focus on heat-resistant substrates, i.e., glass, ceramics, metallic devices, etc. In a classic CVD process, the substrate is exposed to volatile precursors, which react in the CVD-chamber (with the reactive gases) producing the wanted thin layers in the form of amorphous or crystalline coatings. Film coatings by magnetron sputtering (a PVD technique) avoid the high temperatures needed in CVD to decompose the precursors. It has been shown that catalytic/photocatalytic sputtered thin films deposited at temperatures ~130 °C led to uniform and adhesive metal/metal oxides thin-films, showing mechanical interlocking on the chosen substrate. The drawbacks of the CVD deposition method are: (i) the high investment costs; (ii) the high temperatures needed to decompose the precursors and limiting the film deposition on non-heat-resistant surfaces (polymers); and (iii) the costly required cooling systems. Recent developments of sputtering technology led to deposit films presenting high resistance against corrosion and oxidation [23,24]. The coating on multifaceted/complex shapes is one of the greatest problems encountered when preparing thin coatings [25]. HIPIMS applying high electrical pulses induces a strong contact with the textile surfaces or multifaceted structures due to the higher fraction of the achieved metal-ions (M^+) [26]. The strong adhesion of the sputtered atoms/ions/clusters on complex surfaces is due to the higher ions-arrival energies on the surface compared to old method [27].

2. Cu-Coated Textiles: Surface Reactivity, Spectral Absorption and Mechanistic Consideration

Cu-atoms/clusters/ions (hereafter, Cu/CuO_x) were sputtered on cotton/polyester/polyethylene from a 5 cm diameter Cu-target (Lesker AG, Hastings, East Sussex, UK) at a plasma working pressure of 0.1–1 Pa and a deposition current of 0.1–0.3 A. The adhesion of Cu/CuO_x to the surface was strong, such that friction did not allow smearing of the components of the thin film. This is progress with respect to the adhesion of Cu-particles suspensions fixed on pretreated textiles, as recently reported [8]. Deposition time in the seconds/minutes range led to Cu thin films of few nanometer thicknesses on the cotton fabrics. DCMS deposition of Cu/CuO_x led to grey-brown films [28]. Cotton/polyester/polyethylene by itself did not inactivate *Escherichia coli* in the dark or under light. The 40 s Cu-sputtered cotton samples led to complete *E. coli* inactivation within 120 min in the dark and within 30 min under indoor light (~1% of the full solar light irradiation (AM1)). The 180 s Cu-sputtered cotton samples showed a Cu-content of 0.29% Cu wt/wt cotton i.e., five times above the Cu-deposited with 40 s sputtering inactivating the loaded *E. coli* concentration within similar time. This statement is likely due to oxidative action of Cu-ions and not to metallic copper (Cu°). The most favorable structure–reactivity for the Cu-ions/clusters inducing the fastest *E. coli* inactivation was achieved by sputtering Cu/CuO_x for 40 s on the textile surface. The spectral absorption as determined by diffuse reflectance spectroscopy (DRS) showed an increase in the optical absorption as a function of the Cu/CuO_x-sputtering time. The optical absorption range observed for the Cu/CuO_x lies between 200 and 730 nm. The spectral region between 500 and 600 nm shows the inter-band transition of Cu(I). The optical absorption between 600 to 730 nm shows the exciton band and the d-d transition of Cu(II) [29]. By X-ray diffraction, sharp peaks for the Cu/CuO clusters were not observed, since these clusters were not well crystallized due to: (i) the small size of the Cu-nanoparticles attained during this short

sputtering time [20,29]; and (ii) the very low Cu-loading of Cu/CuO_x on cotton fabrics. The Miller (h, k, l) indexing showed peaks corresponding to the face center cubic crystal system (FCC) of the Cu-oxide (111). The signal showed also high noise ratio due to the low Cu-percentage deposited on the textile fabrics [29,30].

Pulsed DCMS (operating at 50 kHz with 15% reversed voltage, a current of 0.3 A and a bias voltage of −400 V) was used to depose Cu/CuO_x on textiles. The negative voltage of −400 V pulsatile switched to 60 V leads to a power density of ~6.5 W/cm^2 accelerating the Cu-atoms/oxides/nanoparticles towards the textile. During the pulsed-DCMS (hereafter, DCMSP), pulses of 10 µs were applied to reduce the overcharge (accumulation of charged species) at the target surface. When the target voltage is pulsed between the usual operating voltage and the ground, the sputtering is termed as unipolar pulsed sputtering. Bipolar pulsed sputtering can also be applied when the target voltage is reversed towards more positive values during the pulse-off period leading to the so-called bipolar asymmetric mode [31].

Sputtering at 0.3 mA using DCMSP for 4 s led to 0.048 wt %Cu/wt-cotton, the threshold loading of Cu for total *E. coli* inactivation. Sputtered samples have been shown to inactivate *E. coli* in the dark within 10 min. This time is shorter compared to the one required by DCMS prepared samples to inactivate *E. coli* under low intensity indoor light (30 min). A Cu-sputtered cotton for 6 s showed a Cu-loading of 0.269 wt %Cu/wt-cotton which is equivalent to about 10^{16} Cu-atoms/cm^2 and a coating thickness of 1.0–1.2 nm (5–6 atomic layers). The DCMSP preparation graft Cu/CuO_x on the cotton or inside the cotton fabric regardless of any agglomeration. This is different to the samples prepared using DCMS where the catalytic activity per atom decreases due to the Cu-nanoparticles agglomeration when sputtered for longer times [28,29].

High power impulse magnetron sputtered (HIPIMS) deposition of Cu on polyester was operated at 100 Hz with pulses of 100 µs separated by 10 ms. The short pulses during the HIPIMS thin film preparation helps to avoid a glow-to-arc transition in the plasma phase during atoms/particles deposition. For 20 s deposition time with 6 A, a thickness of 28 nm was achieved corresponding to 140 Cu-atomic layers. HIPIMS Cu-samples sputtered at 6 A were shown to inactivate *E. coli* when the sputtering has been applied for between 2 and 21 s [32]. The bacterial inactivation took place even in the dark. If we consider the distance between two adjacent Cu-atoms equal to 0.3 nm and the thickness of an atomic layer equal to 0.2 nm, a coating of 20 nm thick is consisted of 100 atomic layers. A film deposited for 20 s with a Cu-deposition rate of 5×10^{15} atom/cm^2·s is consisted of 10^{17} Cu-atom/cm^2.

The antibacterial activity of the Cu-PES prepared by DCMS was evaluated against methicillin resistant *Staphylococcus aureus* (MRSA) [33]. Sputtering Cu on PES for 160 s led to a 3–4 log10 decrease of bacterial load within one hour. Cu-PES might be of use to preclude the transmission of pathogens in hospital facilities if used for beddings, lab-coats, wound dressing... Under light irradiation at wavelengths below 660 nm, copper oxide (CuO_x), a narrow band-gap semi-conductor, undergo charges separation:

$$CuO + light < 660\ nm \rightarrow CuOe^-{}_{cb} + CuO\ h^+{}_{vb} \quad (1)$$

Received photon energies should be within the CuO band-gap energy range. The excited electron reacts directly with O_2 [34–36] leading to $O_2{}^-$ Equation (2) or reducing the Cu^{2+} in the lattice to Cu^+ as noted in Equation (3):

$$CuO(e^-{}_{cb}) + O_2 \rightarrow CuO + O_2{}^- \quad (2)$$

$$CuO(e^-{}_{cb}) \rightarrow (Cu + O^=)^- \quad (3)$$

Bacterial inactivation in anaerobia was recently reported by Rtimi et al. in the dark and under indoor visible light [29]. It was seen that Cu-sputtered polyester (hereafter, PES) inactivates bacteria in the dark under anaerobic conditions. This means that Cu/Cu-ions in contact with the bacteria react in the absence of air (O_2) and are able to inactivate bacteria in the dark. This bacterial inactivation by Cu-species in the dark and/or under anaerobic conditions has been attributed to the translocation/permeation of Cu-ions across the bacterial cell wall. Bacterial reduction mediated

by Cu-NPs has been recently reported in suspensions or on sputtered surfaces [37–42]. We suggest that the bacterial inactivation in the dark on Cu sputtered PES proceeds in air by CuO/$Cu(OH)_2$(NPs) and the production of O_2^- radicals [34,35]. The O_2^- radicals generated in Equation (4) enter the equilibrium described in Equation (5) and lead to the $HO_2^\bullet$ radical and H_2O_2 as noted in Equation (6) [36]:

$$CuO(Cu^+) + O_2 \rightarrow CuO(Cu^{2+}) + O_2^- \quad (4)$$

$$H^+ + O_2^- \Leftrightarrow HO_2^\bullet \text{ (partial } O_2^-) \; pK_a=4.8 \quad (5)$$

$$CuO(Cu^+) + HO_2^\bullet \text{ (partial } {}^\bullet O_2^-) + H^+ \rightarrow CuO(Cu^{2+}) + H_2O_2 \; (k_3= 0.6\text{-}2.3 \; M^{-1}s^{-1}) \quad (6)$$

The initial percentage of Cu and Cu_2O decrease while the percentage of CuO increases during the bacterial inactivation due to the intermediate highly oxidative radicals generated under light irradiation on the Cu PES surface [29]. In the presence of air, O_2^- radicals can be produced [29,34,35]. Figure 1 illustrates bacterial inactivation mechanisms on Cu-PES under aerobic or anaerobic conditions.

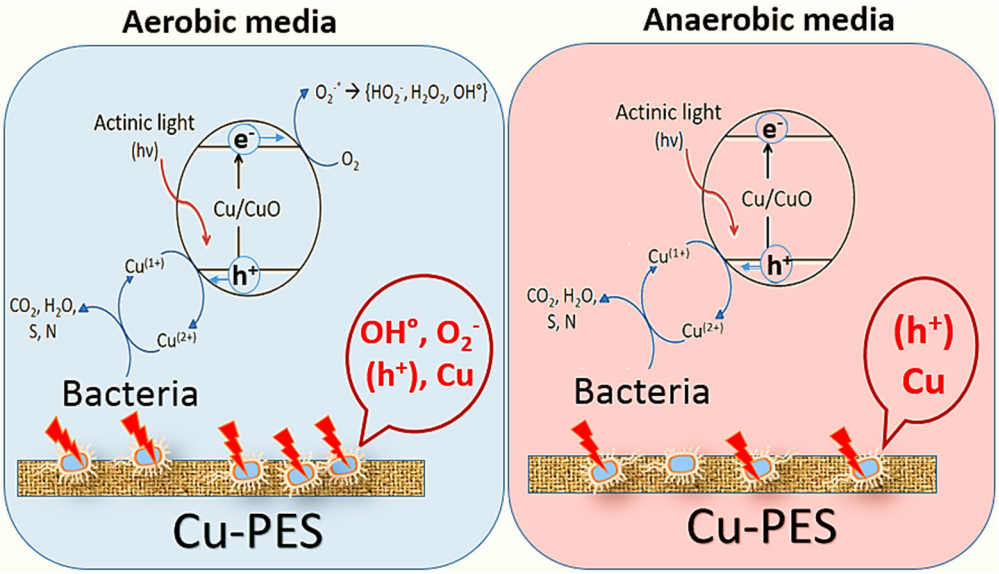

Figure 1. Bacterial inactivation mechanism on Cu/CuO_x sputtered surfaces in aerobic or anaerobic conditions [29].

The reuse of the Cu/CuO_x sputtered surfaces has been reported by Rtimi et al. on different substrates [27,29,30]. Although it seems that in all the tested cases a small amount (few ppb) was seen to be released, the reuse of these samples was quasi-stable for up to 5–8 cycles/reuses. The small Cu-release was attributed to an electrostatic adhesion/interaction between the positively charged Cu-ions (+) and the negatively charged bacterial envelope (−). This release would proceed through an oligodynamic effect to inactivate bacteria. The reuse of these sputtered surfaces suggests their use for medical devices packaging, protective one-use bags, packaging for cells and drug delivery in an exempt environment.

3. TiO_2 Sputtered Thin Films Leading to Bacterial Inactivation: Effect of the Preparation Method

During the last decades, TiO_2 has been used as the golden standard for semiconductor induced infection processes first in solution and later deposited on suitable surfaces, and devices useful in the environmental and health sectors [9,35]. Under band-gap irradiation, the TiO_2 separates the

conduction band electrons (cb(e-)) and valence band holes (vb(h^+)) reacting with O_2 to produce highly oxidative radicals as show in Equation (7).

$$TiO_2 + hV \rightarrow cb(e^-) + vb(h^+) \quad (7)$$

The TiO_2 semiconductor was selected due to it stability, resistance to chemical corrosion and wide availability in purified form. Transparent surfaces are important as wrapping materials in food packaging or as a packaging material of delicate commercial products marketed in the health sector. Polyethylene (PE) has been reported to be a fruitful ground for bacterial incubation and reproduction especially in healthcare facilities (syringe/devices packaging, serum bags, etc.) [43–46]. This was our motivation to develop kinetically fast, stable, robust and adhesive PE-films able to inactivate bacteria/fungi/pathogens under light and/or in the dark. TiO_2 thin films have been deposited on different substrates using colloidal, sol-gel, dip-coating among of other methods [46–49]. These supported TiO_2 films were used for the degradation of coffee, wine, grease and dyes stains on textiles as reported by Rtimi and Kiwi [48]. The same research group investigated also the antibacterial activity of sol-gel and colloidal supported TiO_2 films [44,49]. Although these supported films showed self-cleaning and self-sterilizing activities under UV light, they exhibited low adherence and reproducibility [46,48], their thickness was not controllable and could be easily wiped-off [17,43]. Novel study on TiO_2 supported transparent films involves the use of DCMS to prepare adhesive and uniform/reproducible thin films without damages to the PE fabrics. Due to the surface energy of the PE, it was not possible to depose adhesive coatings with pretreatment of the surface. Rtimi et al. reported the effect of surface pretreatment using plasma and photons enabling adhesive thin coatings [46].

Bacterial inactivation on sputtered TiO_2 films on PE was evaluated under low intensity simulated solar light (assimilated light dose of 52 mW/cm^2). This amount of light was considered as the reasonable amount of light that can reach a room through a glass window during a sunny day at noon. The fastest bacterial inactivation was found for pretreated PE fabrics followed by TiO_2 sputtering for 8 min as reported recently [50]. No significant bacterial inactivation was observed for bacteria on uncoated/bare PE.

A model for bacterial inactivation under light irradiation is proposed in Figure 2, and variations of this model have been generally cited widely for the bacterial disinfection/mineralization mediated by TiO_2 photocatalysis [12,44,46,50]. The intrinsic light absorption by TiO_2 induces the transition 2p (O) → 3d (Ti) as illustrated in Figure 2.

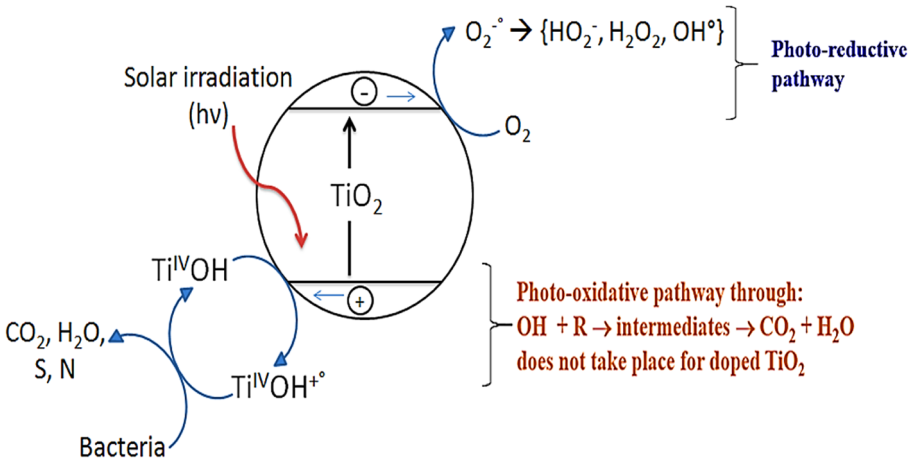

Figure 2. Radicals production by the TiO_2 semiconductor surface under band-gap irradiation.

The photo-generated electrons and holes interact with surface adsorbed molecules such as water and oxygen to form active radicals, so-called reactive oxygen species (ROS). The catalytic reaction of the TiO_2 involves the water, dissolved oxygen and the catalyst surface groups [49,50]. Indeed, they are summarized in Equations (8) and (9):

$$H_2O + vb(h^+) \rightarrow HO^\bullet + H^+ \quad (8)$$

$$O_2 + cb(e\text{-}) \rightarrow O_2^{-\bullet} \quad (9)$$

At the molecular level, the photo-generated electrons tend to reduce Ti^{4+} to Ti^{3+} and the holes react with the bridging oxygen sites leading to oxygen vacancies and free $HO^\bullet$-radicals. Water molecules heal the oxygen vacancies producing OH-groups on the surface leading to the oxidation of Ti^{3+} into Ti^{4+} [49]. The performance of a TiO_2 can be improved by increasing the light absorption in the visible region by doping or coupling with metals/metal oxides hinders the photo-generated charges recombination. This involves the introduction of intra-gap energy level between the cb and vb of TiO_2 facilitating the indirect transition of the electron trough the band gap [36,48,49].

It was recently reported by Rtimi et al. that *E. coli* inactivation kinetics was surprisingly three times faster for the samples prepared by HIPIMS compared to their DCMS counterparts [51]. This fast kinetics was not expected since the TiO_2 prepared via DCMS presents larger nanoparticles size. The TiO_2 released amount (from DCMS samples) was seen to be higher compared to the HIPIMS samples as quantified by inductively coupled plasma mass-spectrometry (ICP-MS). The released Ti-ions do not seem to react through an oligodynamic effect and were observed to diffuse through the less compact thin film prepared by DCMS. The faster bacterial inactivation kinetics observed by the HIPIMS was attributed to the Ti^{4+}/Ti^{3+} redox conversion during bacterial inactivation. This conversion was detected by X-ray photo-electron spectroscopy (XPS) compared to the smaller Ti^{4+}/Ti^{3+} conversion observed for the DCMS-samples. By diffuse reflectance spectroscopy (DRS), a higher optical density was noticed for the HIPIMS samples as shown in Figure 3. The optical absorption of the TiO_2 nano-particles sets in UV range as expected for both samples (DCMS and HIPIMS). Above 400 nm, the DRS spectrum of the PE-TiO_2 HIPIMS sample shows a second component, due to the high energetic particles generated during the HIPIMS deposition on the PE-film. This leads to build up n○π transitions increasing the absorbing sites on the PE [52]. The higher light absorption of the HIPIMS layers provides the evidence for a dense/compact thin film compared to the more transparent TiO_2 layers prepared by DCMS [51].

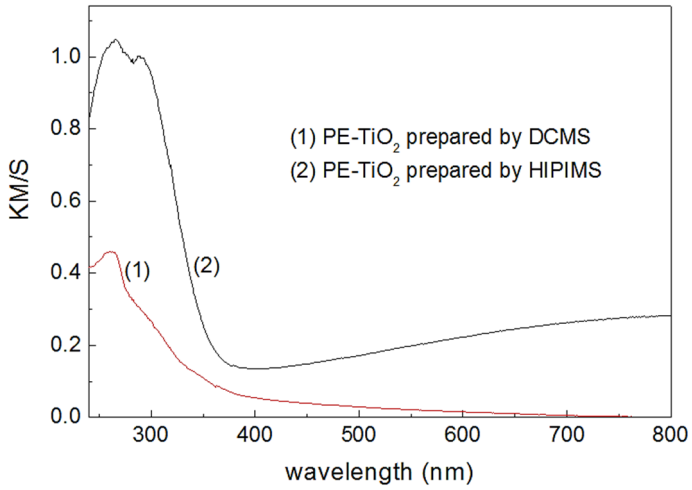

Figure 3. DRS (diffuse reflectance spectroscopy) of PE-TiO_2 prepared by: (1) DCMS (direct current magnetron sputtering) of TiO_2 for 8 min on pretreated-PE; and (2) HIPIMS (High Power Impulse Magnetron Sputtering) of TiO_2 for 4 min on pretreated-PE.

Under band-gap irradiation, highly oxidative HO• radicals were generated on the TiO_2 surface and led to bacterial inactivation as shown in Figure 4. This shows the evidence of the contribution of the photo-generated HO• radicals at the PE-TiO_2 surface leading to bacterial inactivation. These HO• radicals generation was seen to be dependent of sputtering time and the applied light. More recently, Rtimi et al. reported the effect of the applied power/current to the sputtering-target on the HO•-radicals production [51].

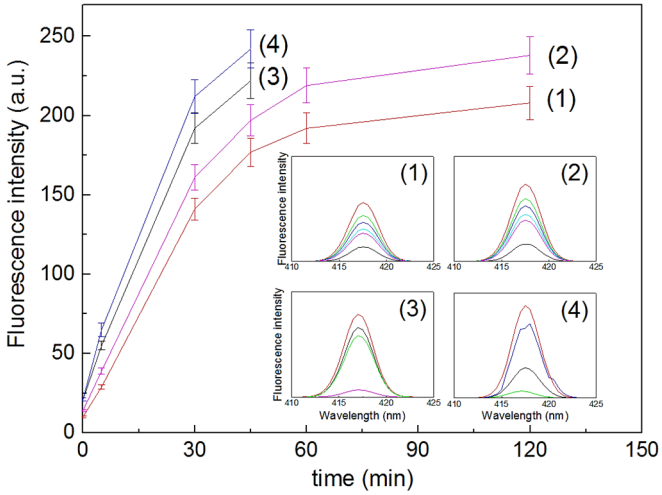

Figure 4. HO•-radical generation from PE-TiO_2 as a function of the temperature (26 and 50 °C) on samples prepared by DCMS (traces 1 and 2) and HIPIMS sputtered samples (traces 3 and 4). Insets show the growth of the fluorescence intensities for DCMS and HIPIMS samples [51].

The increase in HO• radicals generation is proportional to the fluorescence of the 2-hydroxyterephthalic acid and are seen to increase with irradiation time until it reaches a plateau. The HO•-radicals generation was seen to increase by increasing the temperature from 26 to 50 °C. This increase reveals that the process of HO• generation involves ion–molecule, radical–molecule and ion–radical species as recently reported [51–53]. For PE-TiO_2 HIPIMS samples shown in Figure 4 (traces 3 and 4) show alike trend for the generation of HO•-radicals at 26 and 50 °C respectively.

Live/dead stereomicroscopy is a microscopy technique based on kits/stains fluorescence after excitation known wavelengths. A mixture of syto 9 (cell-permeant nucleic acid stain) and propidium iodide can show the physiological state of the bacterial cells, i.e., alive or dead. The physiological state of *E. coli* on TiO_2 sputtered surfaces was investigated in the dark or under light. Only live bacteria were seen on DCMS PE-TiO_2 sputtered samples at zero time as shown in Figure 5a. Gradually membrane damages of bacterial cells appeared at times between 5 min and 45 min illumination as shown by the increasing red dots (dead bacteria). After 120 min irradiation, only dead cells were seen in the stereomicroscopic image. The increase in the outer cell membrane permeability was seen to be responsible for the cell membrane damages [46]. This leads to membrane destabilization not allowing the cell membrane to maintain the osmotic pressure of the bacterial cytoplasm leading eventually to cell death [19,54]. On uncoated PE, *E. coli* cells were seen to stay alive up to 120 min exposure under light. The sample prepared by HIPIMS (see Figure 5b) shows the bacterial physiology up to 45 min under light irradiation.

Bacterial inactivation kinetics for TiO_2 sputtered samples in aerobic and in anaerobic media were recently reported [51]. Obviously, The aerobic media favors the generation of highly oxidative radical and catalytic intermediates. The bacterial inactivation/disinfection in half the time compared to the run under anaerobic conditions was observed on PE-TiO_2 samples. The microoxidation (in terms of pH) at the PE-TiO_2 surface was significant in aerobic media compared to anaerobic media during the bacterial inactivation. The generation of HO_2•-radicals was seen to be more consistent with the

pH- towards more acid values during the disinfection process as previously reported [51]. Figure 6 shows schematically the bacterial inactivation on TiO_2 thin films prepared by HIPIMS compared to the DCMS samples.

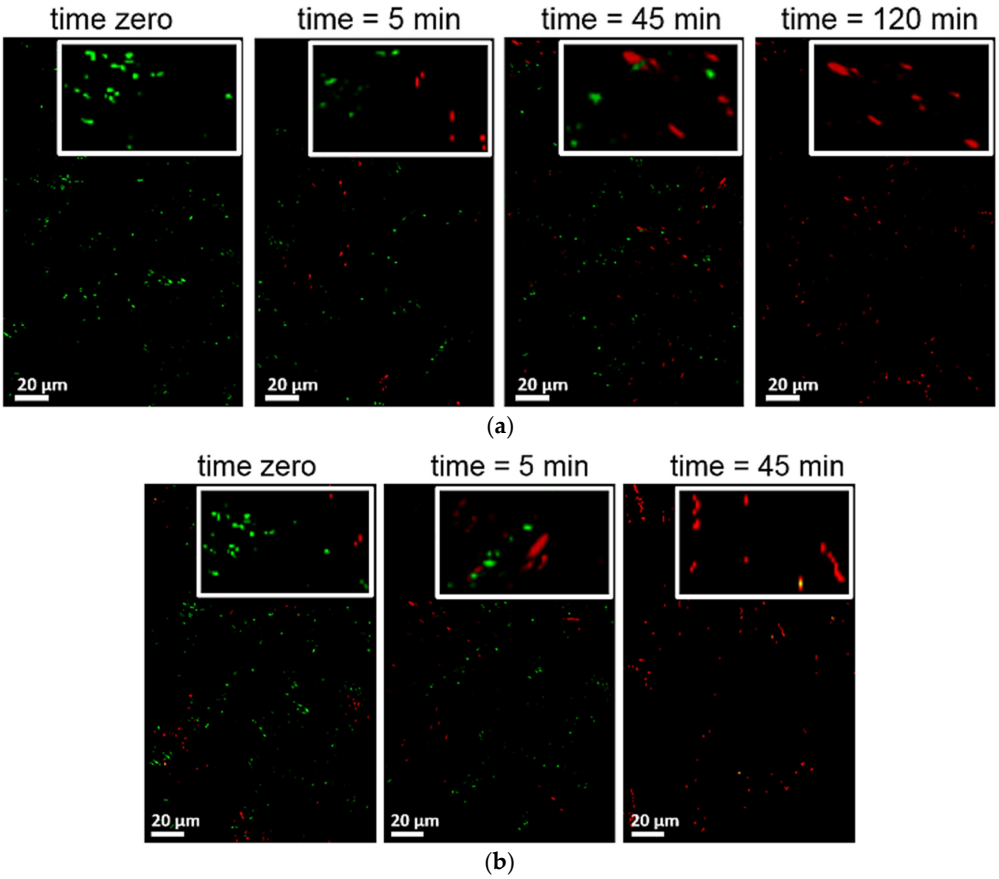

Figure 5. Stereomicroscopy living/dead bacteria irradiated by solar simulated light on: (**a**) PE-TiO_2 DCMS sputtered sample; and (**b**) PE-TiO_2 HIPIMS sputtered sample.

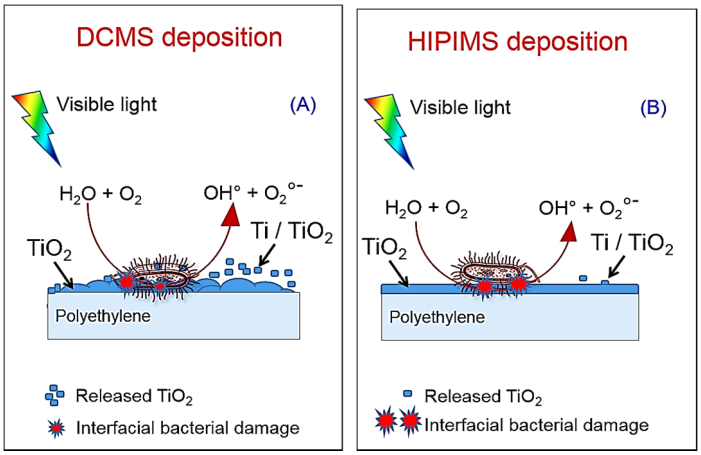

Figure 6. Dynamics of *E. coli* inactivation on compact TiO_2 surfaces prepared by: (A) DCMS and (B) HIPIMS depositions.

Figure 6 shows the dynamic of Ti-release during *E. coli* inactivation process. The less compact DCMS-prepared thin layers release a large amount of Ti-ions as the number of cycles increases as reported by Rtimi et al. [51].

The Ti-ions released during the reuse of samples prepared by DCMS compared to the one prepared by HIPIMS showed more stability of the HIPIMS-samples up to 10 reuse cycles. No significant difference in the released Ti-amounts was observed, suggesting the high coatings adhesivity. However, a difference of a factor of 10 in the Ti-leaching out was observed after the first reuse of the DCMS samples due to the lower compactness of these samples. It was recently reported that the DCMS samples present a higher TiO_2 grain size [51]. The potential use of these transparent and adhesive TiO_2 thin films suggests their use as protective layers on serum bags without hiding the serum/drug level inside the bag. They can also be used for organic products delivery reducing the risk of their contamination. More investigations in the direction of cyto- and eco-toxicity of these coatings have to be addressed for a safer use.

4. Cu Coupled with TiO_2 Sputtered Surfaces Active in the Visible Region: Preparation, Mechanism and Microstructure

The high redox potential Cu nanoparticulate thin films showed fast antibacterial activity. To reduce the amount of Cu released from the sputtered surfaces, we chose to couple it with another photoactive specie, e.g., ZrO_2, TiO_2, TiN, etc. Cu/CuO_x was sputtered with TiO_2 on cotton to evaluate the bacterial loss of viability under visible light or in the dark. The friction with paper or cloth of the deposed mixed thin film did not lead to smearing Ti and/or Cu. This is a development with respect to the adhesion of CuO colloids/nanoparticulates on activated textiles [46].

Copper is more cytotoxic per unit weight compared to silver. This enables tremendously low amounts in the ppb-range of Cu to be used to inactivate bacteria. Innovative thin films made up of CuO_x and TiO_2 sputtered surfaces with similar composition can show distinct atomic scale microstructures according to the way of preparation: (i) sequentially sputtering Ti followed with Cu deposition on the under-layer of TiO_2; or (ii) co-sputtered Ti and Cu. These microstructures can lead to different bacterial inactivation dynamics. Rtimi et al. recently reported the first evidence of the Cu and Ti nanoparticles mapping and distribution on the film surface as detected by wavelength dispersive spectrometry (WDS). They showed the correlation between the surface microstructure and the bacterial inactivation kinetics for the two composite catalyst preventing biofilm formation [55]. For better understanding of the notation, in the present review, we will use CuO_x/TiO_2 for sequentially sputtered surfaces and TiO_2-CuO_x for co-sputtered surfaces.

Baghriche et al. reported the *E. coli* inactivation on TiO_2 deposed for 10 min by DCMS within 2 hours under indoor actinic light (4 mW/cm^2). Cu-sputtered for 40 s by DCMSP inactivated *E. coli* under the same light within 1 hour. When sputtering TiO_2 for 10 min followed by sputtering of Cu-layers for 40 s, the composite film inactivated *E. coli* within less than 5 min under the same light [56] showing the beneficial synergic action of TiO_2 and Cu accelerating the *E. coli* inactivation kinetics. In the dark the *E. coli* inactivation for the sample CuO_x/TiO_2 was reported to occur within 30 min. The release of Cu- and Ti-ions as determined with inductively coupled plasma mass spectrometry (ICP-MS) at a level 6 Cu-ppb and 15 Ti-ppb from the film CuO_x/TiO_2 (10 min/40 s). These small amounts of Cu and Ti are not considered to be cytotoxic for mammalian cells [57] and would proceed through the oligodynamic effect to inactivate bacteria [1]. This involves many enzymes in the mammalian cells neutralizing the small amounts of Ti and Cu. For bacterial cells, the Cu-ions bind electron donor negative groups letting these ions to reach the cytoplasm to disturb the bacterial cell machinery/metabolism [58,59].

The gram negative *E. coli* has a thinner cell wall compared to the gram positive MRSA having a high structural cell wall complexity [12,60]. This difference in wall thickness/microstructure between gram negative and gram positive lead to the different interaction of *E. coli* and MRSA with the photocatalytic surfaces. MRSA is a gram positive bacterium presenting a cell-wall ~40–80 nm thick

with a peptidoglycan content >50%, a lipid content of <3% and no lipo-polysaccharide content. gram negative bacterium *E. coli* presents a cell wall thickness of ~10 nm with a peptidoglycan content of 10%–20%, a lipid content of <58% and a lipo-polysaccharide content of 13%. Kühn et al. reported recently a fast bacterial desinfection of *E. coli* and *P. Aeruginosa* compared to *S. aureus* having a thicker cell wall [61]. Both types of bacteria show a difference in the interaction of with Cu-NPs. This interaction was electrostatically strong between the Cu-NPs/positive-ions with the negative lipopolysaccharide (LPS) outer layer of *E. coli*. This is not the case for the interaction between MRSA and the Cu-NPs positive-ions since both surfaces present similar charges. The adsorption of Cu-NPs on MRSA cell wall has been reported to happen preferentially on the teichoic acid and the peptidoglycan components [62]. For *E. coli* and MRSA, the bacterial desinfection has been reported to occur on several metals/metal oxides [63–65].

Recently, the CuO_x/TiO_2 interfacial charge transfer (IFCT) was reported under solar light (UV-Vis) for a sputtered catalyst. The mechanism of IFCT in CuO_x/TiO_2 and TiO_2-CuO_x leading to bacterial inactivation is summarized in Figure 7.

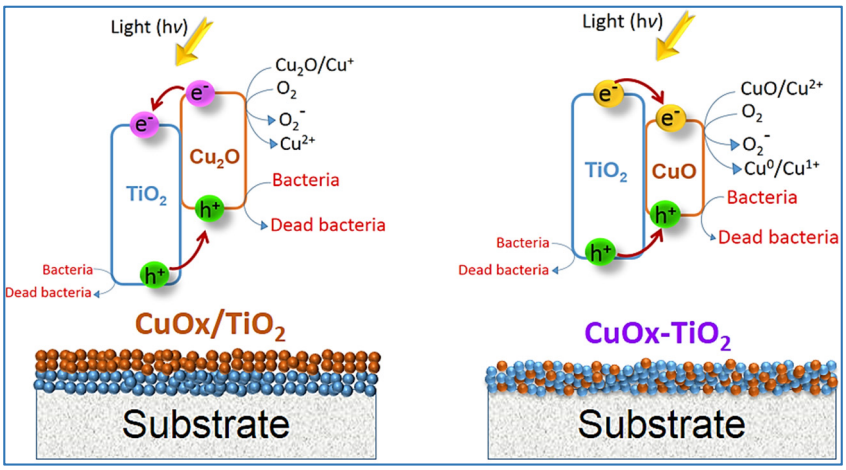

Figure 7. IFCT (interfacial charge transfer) in the system TiO_2 + CuO_x as a function of the preparation procedure.

The band-gap positions [55–57] enable the electronic hole injection from CuO to TiO_2 limiting electron/hole recombination in the CuO and permit the TiO_2 holes (h^+) to inactivate bacteria. The interfacial charge transfer (IFCT) to TiO_2 from the CuO_{vb} at +1.4 eV to the TiO_{2vb} at +2.5 eV vs. SCE was senn to be favorable. the large difference between the two vb levels, leads to the fast *E. coli* inactivation. This difference is considerably drived by pH. These TiO_2vb holes react with the surface –OH of the TiO_2 releasing $HO^{\bullet}$-radicals leading to bacterial oxidation.

To further enhance the bondability of the Cu and Ti on the substrate, HIPIMS deposition was carried out using Cu and TiO_2 targets of 50 mm in diameter (K. Lesker Ltd., East Sussex, UK). A composite TiO_2-CuO_x target with a composition of 60/40 atomic % in TiO_2-CuO_x was also used. The HIPIMS was operated at 500 Hz with pulses of 100 ms separated by 1.9 ms, leading to a deposition rate of TiO_2-CuOx of ~15.3 nm/min. The average power was 87.5 W (5 A, 350 V) and the power per pulse of 100 ms was 1750 W. This deposition was seen to lead to faster bacterial inactivation with lower film thickness. This is a stepwise to save the materials without losing its antibacterial effectiveness.

The bacterial inactivation time versus the film thickness (i.e., amount of material) for DCMS and HIPIMS TiO_2-CuO_x sputtered films [66]. Figure 8 shows the significant reduction for the HIPIMS TiO_2-CuO_x layer thickness compared to DCMS/DCMSP layer required to inactivate bacteria. A thickness of 38 nm was required to inactivate bacteria within ~10 min on the HIPIMS film compared with a thickness layer of 600 nm when applying DCMS/DCMSP. A big difference was also seen

between sequentially sputtered CuOx/TiO_2 (Figure 8, trace 2) and co-sputtered CuOx-TiO_2 (Figure 8, trace 3) with respect to HIPIMS sample (Figure 8, trace 1).

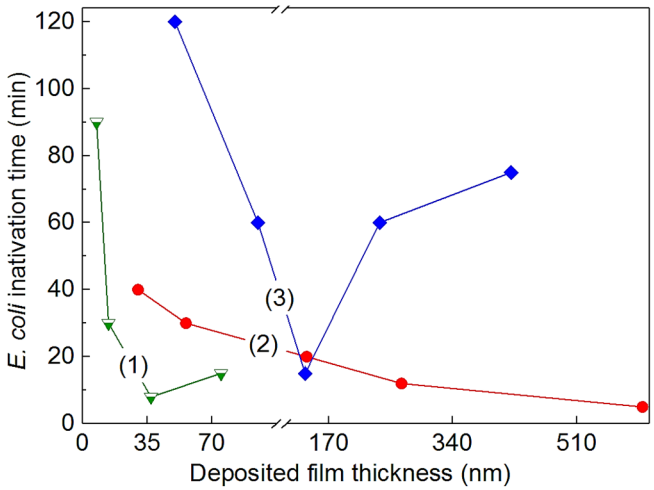

Figure 8. Bacterial inactivation time vs. nominal TiO_2/Cu thicknesses for: (1) HIPIMS deposition (HIPIMS power per pulse was set at 1750 W/100 ms), (2) sequentially sputtered using DCMS deposition [57,67] and (3) co-sputtered using DCMS [66] deposition.

The HIPIMS charge density higher than in DCMSP by two orders of magnitude and comprises pulses ~60 times more energetic than the ones applied by DCMSP [67]. Figure 8 shows that thinner films deposited by HIPIMS exhibit fast bacterial inactivation kinetics. This was attributed to the HIPIMS energy leading to higher ionization percentage $M \rightarrow M^+$ compared to DCMS/DCMSP. These M^+-ions generated in the plasma phase during the HIPIMS deposition migrate and align on the PES surface [66]. The HIPIMS ionization level (generation of M^+) represents about 70% of the sputtered atoms/nanoparticulates with an electronic density of ~10^{19} e^-/m^3 compared to the DCMSP ionization capability estimated at about 5% with an electronic density ~10^{15} e^-/m^3. These positively charged M^+-ions formed in the plasma phase are attracted by the bias voltage applied to the substrate. Figure 8 shows that the fast bacterial inactivation achieved by the samples deposited by HIPIMS (38 nm thick) displays considerable saving of the sputtered species compared to films obtained by conventional DCMS (600 nm thick). HIPIMS deposition induces a strong adhesion at the interface of the substrate due to the higher fraction/energy of the generated Cu- and Ti-ions (M^+) as reported recently [66].

To better understand the structure–reactivity relationship at the interface of the sputtered thin films, etching of the TiO_2-Cu thin film sample sputtered for 150 s was carried out as shown in Figure 9. The latter shows the atomic percent concentration as a function of depth penetration of the etching-ions (generaly Ar-ions). Figure 9 shows that the concentrations of Cu, Ti and O decrease upon the etching of the thin film. The standard value of 15 Ta-atomic layers etched per minute (~30 Å/min) was used as reference to estimated the Ar-etched layers. The Cu-dispersion on the polyester surface shields the Cu-clusters during the *E. coli* inactivation process [57]. The increase in the C-content is attributed to the uncoated PES after removing the TiO_2/Cu coating by etching. The inset in Figure 9 shows the lower atomic concentration percentage of Ti and Cu from TiO_2/Cu sequentially sputtered by DCMS/DCMSP.

Transmission electron microscopy was carried out in a FEI Tecnai TEM-STEM Osiris (200kV, EDX: FEI Super-X; software: Esprit analysis, Bruker Nano). Figure 10 presents in the left hand side TiO_2-Cu imaging showing the Cu-nanoparticles to be immiscible with Ti as contrasted by high angular annular dark field (HAADF). Due to the significant difference in the radii of Cu^{2+} (1.28 Å) and Ti^{4+} (0.53 Å), Cu^{2+} does not substitute Ti^{4+} in the TiO_2 lattice. Due to its size, the CuO/Cu nanoparticles with

particle size >8 nm cannot penetrate bacteria through the cell-wall porins presenting diameters of about 1.2 nm [66]. Only Cu-ions can diffuse through bacterial porins leading to disruption of cell metabolism (DNA damage, interaction with enzymes) leading to the loss of bacterial cultivability and/or viability.

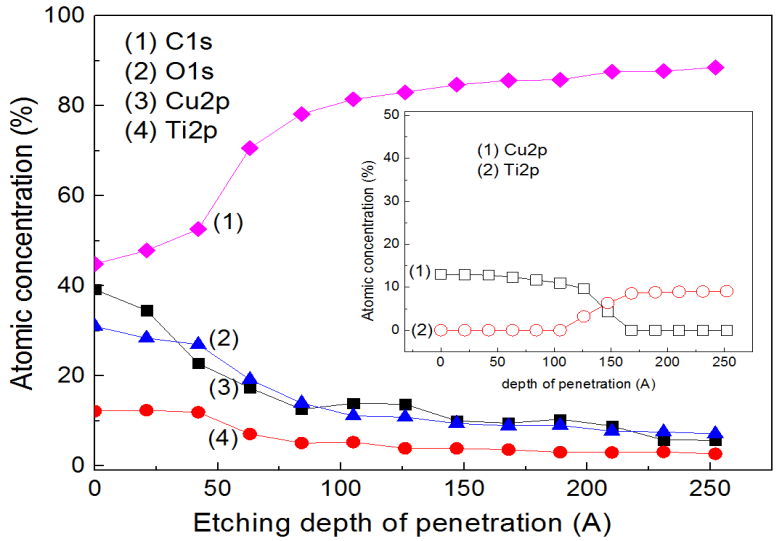

Figure 9. XPS etching of HIPIMS prepared TiO_2-Cu polyester. Inset: Depth profile of sequentially sputtered TiO_2/Cu on polyester prepared by DCMSP [57,66].

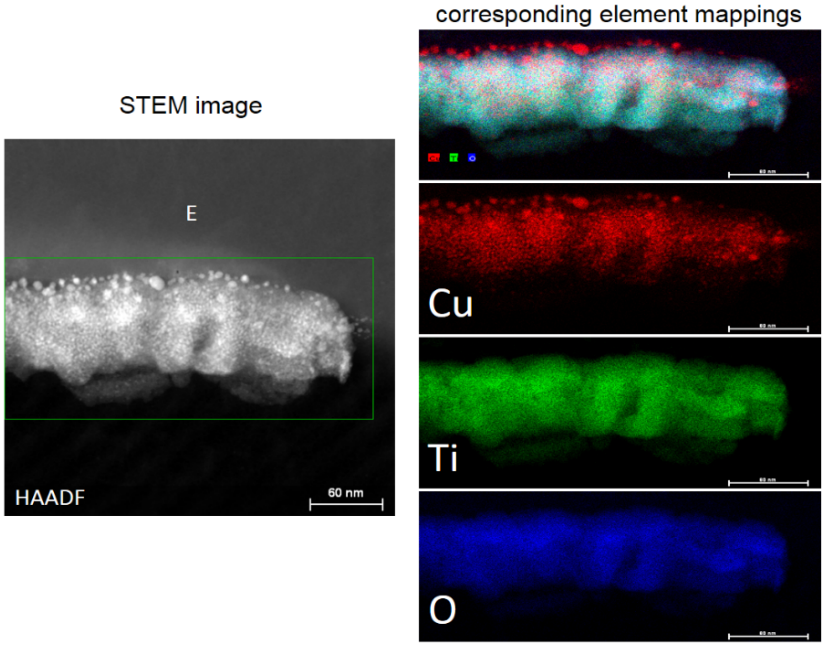

Figure 10. TEM imaging of TiO_2-Cu HIPIMS deposited for 150 s and mapping of Cu, Ti and O [66].

Figure 10 shows the uniform distribution of the Cu and Ti nanoparticles according to their ratio in the sputtered film. Figure 11 shows a schematic charge transfer/transportation in a nano-particulate layer as reported by Snaith et al. [68].

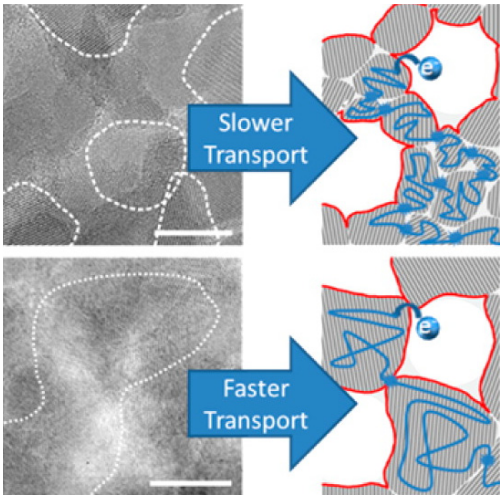

Figure 11. Mobility of conduction band electrons influenced by grain boundaries.

The charge transport is limited by the grains size forming the thin films without taking into account the variability of the inter-particles contact points/area. Snaith et al. observed that the crystal size has a high effect on the electron transfer/transport. This was not solely explicable by considering the relation between free and trapped electrons. Their results are consistent with the long-range mobility of conduction band electrons being strongly influenced by grain boundaries. Consequently, optimizing the crystals/particles size while keeping high enough surface area will be an significant way onward [66–69].

The reuse of TiO_2-Cu and TiO_2/Cu films showed different behaviours related to the adhesivity, the exposed species and the oxidative states at the interface between bacteria and the (photo)catalytic surface. Sequentially sputtered surfaces (TiO_2/Cu) showed stability for up to eight reuses with a Cu-ions release of 15–20 ppb. In the counterpart, co-sputtered TiO_2-Cu showed similar stability with reduced amount of the released species. This suggests the stabilizing effect of the TiO_2 leading to reduced Cu-release compared to sequentially sputtered TiO_2/Cu and Cu/CuO_x sputtered by itself.

5. Conclusions

Controversial mechanisms are reported on the interaction of CuO_x, TiO_2 and CuO_x-TiO_2 with bacterial cells. Spectral shift to the visible region enlarging the light absorption of TiO_2 as a function of the preparation method was also reported. The beneficial effect of Cu on TiO_2 sputtered uniform/adhesive films accelerating bacterial inactivation under indoor visible light was investigated in detail. Cu release in the ppb range was seen to be advantageous for bacterial inactivation in the dark and/or under indoor visible light. A significant saving in metal and energy (deposition time linked to the current and gas consumption) was found by HIPIMS deposition compared to DCMS/DCMSP. This is important due to the increasing demand for Cu, which is rapidly decreasing the known global Cu reserves. Progress in the knowledge of the molecular mechanism implicated in bacteria–TiO_2/Cu interface is needed to design and synthetize more effective antibacterial biomaterial-composites. The oxidative intermediate radicals generated during the photocatalysis degrade/mineralize both types of bacteria independently of the specific bacterial load.

Acknowledgments: I thank the support of the EPFL and the financial support from the Swiss National Science Foundation under Grant No. 2000021-143283/1. I would also like to thank Rosendo Sanjines and César Pulgarin (both at EPFL) for the lab facility and John Kiwi (EPFL) for the valuable discussions.

Conflicts of Interest: The author declares no conflict of interest.

References

1. Bernstein, R.; Freger, V.; Lee, J.; Kim, Y.; Lee, J.; Herzberg, M. 'Should I stay or should I go?' Bacterial attachment vs biofilm formation on surface-modified membranes. *Biofouling* **2014**, *30*, 367–376. [CrossRef] [PubMed]
2. Taylor, K.; Roberts, R.; Roberts, J. *The Challenge of Hospital Acquired Infections (HAI)*; National Audit Office: London, UK, 2002.
3. Plowman, R.; Graves, R.; Griffin, N.; Taylor, L. The rate ad cost of hospital acquired infections. *J. Hosp. Infect.* **2001**, *47*, 198–204. [CrossRef] [PubMed]
4. Dance, S. The role of environmental cleaning in the control of hospital acquired infections. *J. Hosp. Infect.* **2007**, *73*, 378–389. [CrossRef] [PubMed]
5. Kramer, A.; Schwebke, I.; Kampf, G. How long do nosocomial pathogens persist on inanimate surfaces? *Diseases* **2006**, *6*, 137–146.
6. Borkow, G.; Gabbay, J. Puttting copper into action. Copper impregnated products with potental biocidal activities. *J. FASEB* **2008**, *18*, 1728–1730.
7. Borkow, G.; Gabbay, J. Biocidal Textiles can help fight nosocomial infections. *Med. Hypothesis* **2008**, *70*, 990–994. [CrossRef] [PubMed]
8. Torres, A.; Ruales, C.; Pulgarin, C.; Aimable, A.; Bowen, P.; Kiwi, J. Innovative High-Surface-Area CuO pretreated Cotton Effective in Bacterial Inactivation under Visible Light. *Appl. Mater. Interfaces* **2010**, *2*, 2547–2552. [CrossRef] [PubMed]
9. Kiwi, J.; Pulgarin, C. Innovative self-cleaning and bactericide textiles. *Catal. Today* **2010**, *151*, 2–7. [CrossRef]
10. Pigeot-Rémy, S.; Simonet, F.; Errazuriz-Cerda, E.; Lazzaroni, E.; Atlan, D.; Guillard, C. Photocatalysis and disinfectionof water: Identification of potential bacterial targets. *Appl. Catal. B* **2011**, *201*, 390–398. [CrossRef]
11. Markowska-Szczupak, A.; Ulfig, K.; Morawski, A. The application of TiO_2 for deactivation of bioparticules: An overview. *Catal. Today* **2011**, *169*, 249–257. [CrossRef]
12. Foster, H.; Ditta, I.; Varghese, S.; Steele, A. Photocatalytic disinfection using titanium dioxide: Spectrum and mechanism of antimicrobial activity. *Appl. Microbiol. Biotech.* **2010**, *90*, 1847–1868. [CrossRef] [PubMed]
13. Applerot, G.; Abu-Mukh, R.; Irzh, R.; Charmet, J.; Keppner, J.; Laux, L.; Guilbert, G.; Gedanken, A. Decorative parylene coated glass with ZnO nanoparticles for antibacterial applications. *ACS Appl. Mater. Interfaces* **2010**, *2*, 1052–1059. [CrossRef] [PubMed]
14. Perelshtein, I.; Applerot, N.; Perkas, N.; Wehrshuetz-Sigl, E.; Hasman, E.G.; Guebitz, G.; Gedanken, A. CuO-cotton nanocomposite: Formation, Morphology and bacterial activity. *Surf. Coat. Technol.* **2009**, *204*, 54–57. [CrossRef]
15. Yuranova, T.; Rincon, G.; Bozzi, A.; Parra, S.; Pulgarin, C.; Albers, P.; Kiwi, J. Antibacterial textiles prepared by RF-plasma and vacuum-UV mediated deposition of silver. *J. Photochem. Photobiol. A Chem.* **2003**, *161*, 27–34. [CrossRef]
16. Yuranova, T.; Rincon, G.; Pulgarin, C.; Laub, D.; Xanthopoulos, N.; Mathieu, H.-J.; Kiwi, J. Bactericide cotton textiles active in *E coli* abatement prepared under mild preparation conditions. *J. Photochem. Photobiol. A* **2006**, *181*, 363–369. [CrossRef]
17. Zhang, L.; Dillert, R.; Bahnemann, D. Photoinduced hydrophylicity and self-cleaning: Models and reality. *Energy Environ. Sci.* **2012**, *5*, 7491–7507. [CrossRef]
18. Mills, A.; Hill, P.; Robertson, P. Overview of the current ISO tests for photocatalytic materials. *J. Photochem. Photobiol. A* **2012**, *237*, 7–23. [CrossRef]
19. Page, K.; Wilson, W.; Parkin, I.P. Antimicrobial surfaces and their potential in reducing the role of the inanimate environment in the incidence of hospital-acquired infections. *J. Mater. Chem.* **2009**, *19*, 3819–3831. [CrossRef]
20. Foster, H.A.; Sheel, P.; Sheel, D.W.; Evans, P.; Varghese, S.; Rutschke, N.; Yates, H.M. Antimicrobial activity of titatnia/silver and titania/copper films prepared by CVD. *J. Photochem. Photobiol. A* **2010**, *216*, 283–289. [CrossRef]
21. Dunlop, P.S.M.; Sheeran, C.P.; Byrne, J.A.; McMahon, M.A.S.; Boyle, M.A.; McGuigan, K.G. Inactivation of clinically relevant pathogens by photocatalytic coatings. *J. Photochem. Photobiol. A* **2010**, *216*, 303–310. [CrossRef]

22. Yates, M.H.; Brook, L.A.; Ditta, I.B.; Evans, P.; Foster, A.H.; Sheel, W.D.; Steele, A. Photo-induced self–cleaning and biocidal behviour of titania and copper oxide multilayers. *J. Photochem. Photobiol. A* **2008**, *197*, 197–208. [CrossRef]
23. Sarakinos, K.; Alami, J.; Konstantinidis, D. High power pulsed magnetron sputtering: A review on scientific and engineering state of the art. *Surf. Coat. Technol.* **2010**, *204*, 1661–1684. [CrossRef]
24. Lin, J.; Moore, J.; Sproul, W.; Mishra, B.; Wu, Z.; Wang, L. The structure and properties of chromium nitride coatings deposited using dc, pulsed dc and modulated pulse power magnetron sputtering. *Surf. Coat. Technol.* **2010**, *204*, 2230–2239. [CrossRef]
25. Alami, J.; Persson, P.; Gudmunsson, P.; Bohlmark, J.; Helmersson, J. Ion-assisted physical vapor deposition for enhanced film properties on nonflat surfaces. *J. Vac. Technol. A* **2005**, *23*, 278–280. [CrossRef]
26. Kelly, J.P.; Arnell, D.R. Magnetron sputtering: A review of recent developments and applications. *Vacuum* **2000**, *56*, 159–172. [CrossRef]
27. Rtimi, S.; Sanjines, R.; Pulgarin, C.; Kiwi, J. Quasi-Instantaneous Bacterial Inactivation on Cu-Ag Nano-particulate 3D-Catheters in the Dark and Under Light: Mechanism and Dynamics. *ACS Appl. Mater. Interfaces* **2016**, *8*, 47–55. [CrossRef] [PubMed]
28. Castro, C.; Pulgarin, C.; Osorio, P.; Giraldo, S.; Kiwi, J. Structure-reactivity relations of the Cu-cotton sputtered layers during *E. coli* inactivation in the dark and under light. *J. Photochem. Photobiol. A* **2010**, *216*, 295–302. [CrossRef]
29. Rtimi, S.; Sanjines, R.; Pulgarin, C.; Kiwi, J. Effect of Light and Oxygen on repetitive bacterial inactivation on uniform, adhesive, robust and stable Cu-polyester surfaces. *J. Adv. Oxid. Technol.* **2017**. [CrossRef]
30. Rtimi, S.; Sanjines, R.; Bensimon, M.; Pulgarin, C.; Kiwi, J. Accelerated *Escherichia coli* inactivation in the dark on uniform copper flexible surfaces. *Biointerphases* **2014**, *9*, 029012. [CrossRef] [PubMed]
31. Osorio, P.; Sanjines, R.; Ruales, C.; Castro, C.; Pulgarin, C.; Rengifo, J.-A.; Lavanchy, J.-C.; Kiwi, J. Antimicrobial Cu-functionalized surfaces prepared by bipolar asymmetric DC-pulsed magnetron sputtering (PMS). *J. Photochem. Photobiol. A* **2011**, *220*, 70–76. [CrossRef]
32. Kusiak-Nejman, E.; Morawski, A.; Ehiasarian, A.; Baghriche, O.; Pulgarin, C.; Mielczarski, E.; Mielczarski, J.; Kulik, A.; Kiwi, J. *E. coli* Inactivation by High Power Impulse Magnetron Sputtered (HIPIMS) Cu-Surfaces. *J. Phys. Chem. C* **2011**, *115*, 21113–21119. [CrossRef]
33. Rio, L.; Kusiak, E.; Kiwi, J.; Pulgarin, C.; Trampuz, A.; Bizzini, A. Comparative methods to evaluate the bactericidal activity of copper-sputtered surfaces against methicillin-resistant *staphylococcus aureus*. *J. Appl. Microbiol.* **2012**, *78*, 8176–8182. [CrossRef] [PubMed]
34. Hardee, K.; Bard, J. Semiconductor electrodes: X. Photochemical behavior of polycrystalline metal-oxides electrodesin aqueous solutions. *J. Electrochem. Soc.* **1977**, *124*, 215–224. [CrossRef]
35. Kiwi, J.; Rtimi, S.; Pulgarin, C. Cu, Cu/TiO_2 thin films sputtered by up to date methods on non-thermal thin resistant substrates leading to bacterial inactivation. In *Microbial Pathogens and Strategies for Combating Them: Science, Technology and Education*; Méndez-Vilas, A., Ed.; Formatex Research Center: Extremadura, Spain, 2013; Volume 1, pp. 74–82.
36. Bandara, J.; Guasaquillo, I.; Bowen, P.; Soare, L.; Jardim, W.; Kiwi, J. Photocatalytic Storing of O_2 as H_2O_2 Mediated by High Surface Area CuO. Evidence for the Reductive-Oxidative Interfacial Mechanism of Reaction. *Langmuir* **2005**, *21*, 8554–8559. [CrossRef] [PubMed]
37. Sunada, K.; Watanabe, S.; Hashimoto, K. Bactericidal Activity of Copper Deposited TiO_2 Film under UV Light Illumination. *Environ. Sci. Technol.* **2003**, *40*, 4785–4789. [CrossRef]
38. Ishiguro, H.; Yao, Y.; Nakano, Y.; Hara, M.; Sunada, K.; Hashimoto, K.; Kajioka, J.; Fujishima, A.; Kubota, Y. Photocatalytic activity of Cu^{2+}/TiO_2-coated cordierite foam inactivates bacteriophages and *Legionella pneumophila*. *Appl. Catal. B* **2013**, *129*, 56–61. [CrossRef]
39. Ditta, I.B.; Steele, A.; Liptrot, C.; Tobin, J.; Tyler, H.; Yates, H.M.; Sheel, D.W.; Foster, H.A. Photocatalytic antimicrobial activity of thin surface films of TiO_2, CuO and TiO_2/CuO dual layers on *Escherichia coli* and bacteriophage T_4. *Appl. Microbiol. Biotechnol.* **2008**, *79*, 127–133. [CrossRef] [PubMed]
40. Irie, H.; Miura, S.; Kamiya, S.; Hashimoto, K. Efficient visible light-sensitive photocatalysis: Grafting Cu(II) ions onto TiO_2 and WO_3 photocatalysts. *Chem. Phys. Letts.* **2008**, *457*, 202–205. [CrossRef]
41. Qiu, X.; Miyauchi, M.; Sunada, K.; Minoshima, M.; Liu, M.; Lu, Y.; Ding, L.; Shomodaira, Y.; Hosogi, Y.; Kuroda, Y.; et al. Hybrid Cu_xO/TiO_2 Nanocomposites As Risk-Reduction Materials in Indoor Environments. *ACS Nano* **2012**, *6*, 1609–1618. [CrossRef] [PubMed]

42. Li, J.; Dennehy, J. Differential Bacteriophage Mortality on Exposure to Copper. *Appl. Environ. Microbiol.* **2011**, *77*, 6878–6883. [CrossRef] [PubMed]
43. Rtimi, S.; Pulgarin, C.; Sanjines, R.; Kiwi, J. Kinetics and mechanism for transparent polyethylene-TiO_2 films mediated self-cleaning leading to MB dye discoloration under sunlight irradiation. *Appl. Catal. B Environ.* **2015**, *162*, 236–244. [CrossRef]
44. Nesic, J.; Rtimi, S.; Laub, D.; Roglic, G.M.; Pulgarin, C.; Kiwi, J. New evidence for TiO_2 uniform surfaces leading to complete bacterial reduction in the dark: Critical issues. *Colloids Surf. B Biointerfaces* **2014**, *123*, 593–599. [CrossRef] [PubMed]
45. Kiwi, J.; Rtimi, S.; Nesic, J.; Pulgarin, C.; Sanjines, R.; Bensimon, M.; Kiwi, J. Effect of surface pretreatment of TiO_2 films on interfacial processes leading to bacterial inactivation in the dark and under light irradiation. *Interface Focus* **2014**, *5*, 20140046.
46. Rtimi, S.; Sanjines, R.; Andrzejczuk, M.; Pulgarin, C.; Kulik, A.; Kiwi, J. Innovative transparent non-scattering TiO_2 bactericide thin films inducing increased *E. coli* cell wall fluidity. *Surf. Coat. Technol.* **2014**, *254*, 333–343. [CrossRef]
47. Petronella, F.; Rtimi, S.; Comparelli, R.; Sanjines, R.; Pulgarin, C.; Curri, M.L.; Kiwi, J. Uniform TiO_2/In_2O_3 surface films effective in bacterial inactivation under visible light. *J. Photochem. Photobiol. A Chem.* **2014**, *279*, 1–7. [CrossRef]
48. Kiwi, J.; Rtimi, S. Environmentally mild self-cleaning processes on textile surfaces under daylight irradiation: Critical issues. In *Active Coatings for Smart Textiles*; Hu, J., Ed.; Elsevier Limited: Amsterdam, The Netherlands, 2016.
49. Baghriche, O.; Rtimi, S.; Pulgarin, C.; Roussel, C.; Kiwi, J. RF-plasma pretreatment of surfaces leading to TiO_2 coatings with improved optical absorption and OH-radical production. *Appl. Catal. B Environ.* **2013**, *130–131*, 65–72. [CrossRef]
50. Rtimi, S.; Pulgarin, C.; Sanjines, R.; Kiwi, J. Innovative semi-transparent nanocomposite films presenting photo-switchable behavior and leading to a reduction of the risk of infection under sunlight. *RSC Adv.* **2013**, *3*, 16345–16348. [CrossRef]
51. Rtimi, S.; Giannakis, S.; Bensimon, M.; Pulgarin, C.; Sanjines, R.; Kiwi, J. Supported TiO_2 films deposited at different energies: Implications of the surface compactness on the catalytic kinetics. *Appl. Catal. B Environ.* **2016**, *191*, 42–52. [CrossRef]
52. Chan, C.; Ko, T.; Hiroaka, N. Polymer surface modification by plasma and photons. *Surf. Sci. Rep.* **1996**, *24*, 1–54. [CrossRef]
53. Winkler, J. *Titanium Oxide*; Vincentz: Hannover, Germany, 2003.
54. Page, K.; Palgrave, R.G.; Parkin, I.P.; Wilson, M.; Savin, P.S.L.; Chadwick, V.A. Titania and silver titania composite films on glass antimicrobial coating. *J. Mater. Chem.* **2007**, *17*, 95–104. [CrossRef]
55. Rtimi, S.; Robyr, M.; Pulgarin, C.; Lavanchy, J.-C.; Kiwi, J. A New Perspective in the Use of FeO_x-TiO_2 Photocatalytic Films: Indole Degradation in the Absence of Fe-Leaching. *J. Catal.* **2016**, *342*, 184–192. [CrossRef]
56. Baghriche, O.; Rtimi, S.; Sanjines, R.; Pulgarin, C.; Kiwi, J. Effect of the spectral properties of TiO_2, Cu, TiO_2/Cu sputtered films on the bacterial inactivation under low intensity actinic light. *J. Photochem. Photobiol. A* **2013**, *251*, 50–56. [CrossRef]
57. Baghriche, O.; Rtimi, S.; Pulgarin, C.; Sanjines, R.; Kiwi, J. Innovative TiO_2/Cu Nanosurfaces Inactivating Bacteria in the Minute Range under Low-Intensity Actinic Light. *ACS Appl. Mater. Interfaces* **2012**, *4*, 5234–5240. [CrossRef] [PubMed]
58. Negishi, N.; Iyoda, T.; Hashimoto, K.; Fujishima, A. Preparation of Transparent TiO_2 Thin Film Photocatalyst and Its Photocatalytic Activity. *Chem. Lett.* **1995**, *24*, 841–842. [CrossRef]
59. Nikaido, H.J. Prevention of Drug Access to Bacterial Targets. Permeability Barriers and Active Flux. *Biol. Chem.* **1994**, *269*, 3905–3909.
60. Pelaez, M.; Nolan, N.; Pillai, S.; Seery, M.; Falaras, P.; Kontos, A.; Dunlop, P.S.M.; Hamilton, J.; Byrne, J.-A.; O'Shea, K.; et al. A Review on the Visible Light Active Titanium Dioxide Photocatalysts for Environmental Applications. *Appl. Catal. B* **2012**, *125*, 331–349. [CrossRef]
61. Kühn, K.; Chaberny, I.; Massholder, K.; Sticker, M.; Benz, V.; Sonntag, V.H.-G.; Erdinger, I. Disinfection of surfaces by photocatalytic oxidation with titanium dioxide and UVA light. *Chemosphere* **2003**, *53*, 71–77. [CrossRef]

62. Espirito Santo, C.; Lam, E.; Elowsky, C.; Quarnta, D.; Domaille, D.; Chang, C.; Grass, G. Bacterial Killing by Dry Metallic Copper Surfaces. *Appl. Environ. Microbiol.* **2011**, *77*, 794–802. [CrossRef] [PubMed]
63. Rentz, E. Viral Pathogens and Severe Acute Respiratory Syndrome: Oligodynamic Ag^{+} for Direct Immune Intervention. *J. Nutr. Environ. Med.* **2003**, *13*, 109–118. [CrossRef]
64. Thill, A.; Zeyons, O.; Spalla, O.; Chauvat, F.; Rose, J.; Auffan, M.; Flank, A.-M. Cytotoxicity of CeO_2 Nanoparticles for *Escherichia coli.* Physico-Chemical Insight of the Cytotoxicity Mechanism. *Environ. Sci. Technol.* **2006**, *40*, 6151–6156. [CrossRef] [PubMed]
65. Nadtochenko, V.; Rincon, G.; Stanka, S.; Kiwi, J. Dynamics of *E. coli* membrane cell peroxidation during TiO_2 photocatalysis studied by ATR-FTIR spectroscopy and AFM microscopy. *J. Photochem. Photobiol. A* **2005**, *169*, 131–137. [CrossRef]
66. Rtimi, S.; Baghriche, O.; Pulgarin, C.; Lavanchy, J.-C.; Kiwi, J. Growth of TiO_2/Cu films by HiPIMS for accelerated bacterial loss of viability. *Surf. Coat. Technol.* **2013**, *232*, 804–813. [CrossRef]
67. Rtimi, S.; Ballo, M.; Laub, D.; Pulgarin, C.; Entenza, J.; Bizzini, A.; Sanjines, R.; Kiwi, J. Duality in the *Escherichia coli* and methicillin resistant *Staphylococcus aureus* reduction mechanism under actinic light on innovative co-sputtered surfaces. *Appl. Catal. A Gen.* **2015**, *498*, 185–191. [CrossRef]
68. Docampo, P.; Guldin, S.; Steiner, U.; Snaith, H.J. Charge Transport Limitations in Self-Assembled TiO_2 Photo-anodes for Dye-Sensitized Solar Cells. *J. Phys. Chem. Lett.* **2013**, *4*, 698–703. [CrossRef] [PubMed]
69. Alhussein, A.; Achache, S.; Deturche, R.; Sanchette, F.; Pulgarin, C.; Kiwi, J.; Rtimi, S. Beneficial effect of Cu on Ti-Nb-Ta-Zr sputtered uniform/adhesive gum films accelerating bacterial inactivation under indoor visible light. *Collids Surf. B Biointerface* **2017**, *152*, 152–158. [CrossRef] [PubMed]